Available online at www.sciencedirect.com

SCIENCE DIRECT®

ELSEVIER

Journal of Sound and Vibration 285 (2005) 1223–1234

JOURNAL OF SOUND AND VIBRATION

www.elsevier.com/locate/jsvi

Short Communication

Transient responses of a 2-dof torsional system with nonlinear dry friction under a harmonically varying normal load

Chengwu Duan, Rajendra Singh*

Acoustics and Dynamics Laboratory, Department of Mechanical Engineering and The Center for Automotive Research, The Ohio State University, 650 Ackerman Road, Columbus, OH 43202, USA

Received 1 November 2004; accepted 10 November 2004
Available online 18 January 2005

Abstract

The effects of a harmonically varying normal load on transient responses of a two-degree-of-freedom torsional system, with nonlinear dry friction and under sinusoidal torque excitation, are reported. An approximate analytical solution for pure slip-type transients is first obtained and confirmed with computational studies. Although the negative slope in friction–velocity characteristics introduces substantial stick-slip motions, a well-tuned normal load could possibly attenuate such motions. Key parameters controlling the engagement rate are identified.
© 2004 Elsevier Ltd. All rights reserved.

1. Introduction

Recently, Duan and Singh examined the nonlinear dynamics of a two-degree-of-freedom (2-dof) torsional system with a dry friction controlled path and found significant stick-slip motions [1,2]. However, the prior studies assumed a constant normal load N. In this communication, we investigate the effect of time-varying N for the same torsional system. An immediate application of this work is the slipping torque converter clutch (TCC) that is employed in an automotive driveline system, as illustrated in Fig. 1(a). Unlike a pure dry friction damper that has been examined by many researchers [3–5], the dry friction element of Fig. 1(a) is used as a key path to

*Corresponding author. Tel.: +1 614 292 9044; fax: +1 614 292 3163.
E-mail address: singh.3@osu.edu (R. Singh).

0022-460X/$ - see front matter © 2004 Elsevier Ltd. All rights reserved.
doi:10.1016/j.jsv.2004.11.004

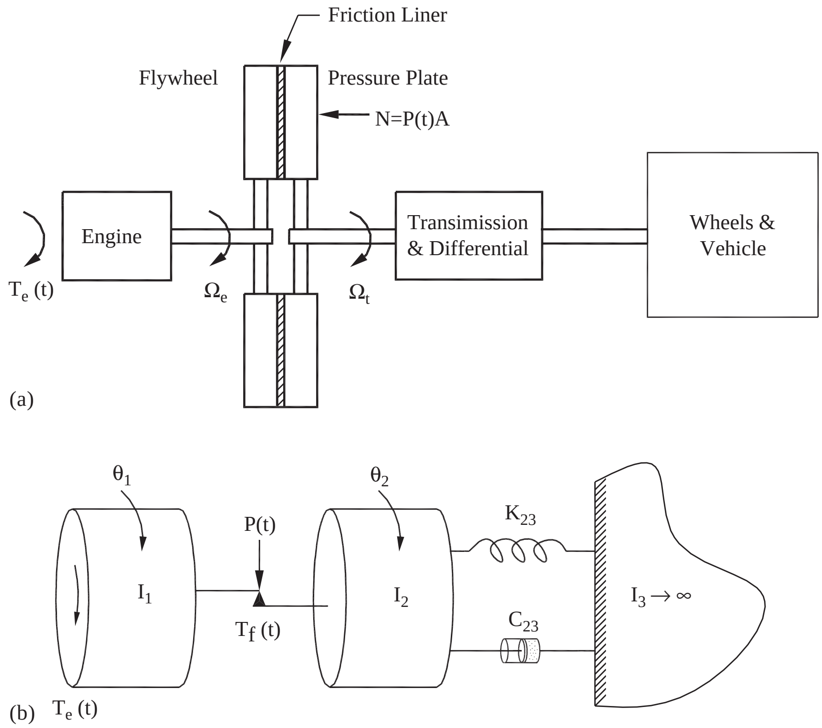

Fig. 1. Torsional systems with dry friction element. (a) Automotive driveline system with torque converter clutch; (b) schematic of a 2-dof system.

transmit the mechanical power. The nonlinear friction torque T_{sf} is applied by an actuation pressure $P(t)$, and in this study, we assume $P(t)$ to be harmonic along with a mean term. Fig. 1(b) shows the schematic representation of a reduced automotive driveline system. Here, I_1 represents the combined torsional inertia of a flywheel, I_2 is the inertia of the friction shoe and pressure plate, I_3 is the wheel and vehicle sub-system that is assumed to be rigid. The governing equations for this system are

$$I_1\ddot{\theta}_1 + T_f(\dot{\theta}_1 - \dot{\theta}_2, t) = T_e(t) = T_m + T_p \sin(\omega t), \tag{1a}$$

$$I_2\ddot{\theta}_2 + C_{23}\dot{\theta}_2 + K_{23}\theta_2 = T_f(\dot{\theta}_1 - \dot{\theta}_2, t). \tag{1b}$$

Here, θ_1 are θ_2 are absolute angular displacements; C_{23} and K_{23} are the lumped viscous damping and stiffness associated with the automotive driveline. The engine torque excitation $T_e(t)$ is composed of mean $T_m = \langle T_e \rangle_t$ and pulsating T_p components, where $\langle\rangle_t$ is the time-average operator. When relative motions are of interest, rewrite Eq. (1), where $\delta_1 = \theta_1 - \theta_2$ and $\delta_2 = \theta_2$:

$$I_1\ddot{\delta}_1 - \frac{I_1}{I_2}C_{23}\dot{\delta}_2 - \frac{I_1}{I_2}K_{23}\delta_2 + \left(1.0 + \frac{I_1}{I_2}\right)T_f(\dot{\delta}_1, t) = T_m + T_p \sin(\omega t), \tag{2a}$$

$$I_2\ddot{\delta}_2 + C_{23}\dot{\delta}_2 + K_{23}\delta_2 = T_f(\dot{\delta}_1, t). \tag{2b}$$

2. Nonlinear time-varying dry friction formulation

The nonlinear friction torque $T_f(\dot{\delta}_1, t)$ is carried by the clutch and then it acts as an equivalent torque excitation to the downstream system. In a realistic automotive system, a pulse-width-modulated solenoid valve would generate $P(t)$ by changing the command value or duty ratio [6,7]. That results in a nonlinear time-varying (NLTV) friction torque formulation, $T_f(\dot{\delta}_1, t) = \mu(\dot{\delta}_1)P(t)AR$, where μ is the velocity-dependent coefficient of friction. Note that A and R are pressure area and moment arm and they are assumed to be time-invariant. Express the $P(t)$ profile in the form of a sinusoidal signal with mean pressure P_m, amplitude P_p, starting time t_0 and the actuation pressure frequency ω_f:

$$P(t) = \begin{cases} 0, & t < t_{0-}, \\ P_m + P_p \sin(\omega_f t + \psi), & t \geqslant t_{0+}. \end{cases} \tag{3}$$

Here, ψ is the phase lag between the actuation pressure and $T_e(t)$. In this study, we set the initial engagement time at $t_{0+} = 0$ without loss of generality and $P(t)$ is assumed to be positive-definite to ensure that no separation occurs across the frictional interface, i.e. $P_p/P_m \in [0, 1)$. The following friction formulation $\mu(\dot{\delta}_1)$ is employed, since the aim of this study is to examine the phenomenological dynamic behavior [8]:

$$\mu(\dot{\delta}_1) = \begin{cases} \left[\mu_k + (\mu_s - \mu_k)\mathrm{e}^{-\alpha|\dot{\delta}_1|}\right]\mathrm{sgn}(\dot{\delta}_1), & |\dot{\delta}_1| > 0, \\ [0\ \mu_s], & \dot{\delta}_1 = 0. \end{cases} \tag{4}$$

Here, α is a positive constant that controls the gradient of μ with respect to $\dot{\delta}_1$; μ_s is the static friction coefficient; μ_k is the kinetic friction coefficient and sgn is the conventional triple-valued signum function. In our study, $\alpha = 2$ is chosen for the sake of illustration. To further reduce the system parameters, we could incorporate μ_k, A and R within $P(t)$ to yield the NLTV friction torque $T_f(\dot{\delta}, t)$ as

$$T_f(\dot{\delta}, t) = \bar{\mu}(\dot{\delta}_1)T_s(t), \quad T_s(t) = \mu_k A\ R\ P(t) = T_{sm} + T_{sp}\sin(\omega_f t + \psi). \tag{5a,b}$$

Here, $\bar{\mu}(\dot{\delta}_1)$ has been normalized with respect to μ_k. Further, the sign function of Eq. (4) is smoothened by a hyper-tangent function to facilitate the numerical integration [9] for the nonlinear stick-slip motions:

$$\bar{\mu}(\dot{\delta}_1) = \left[1.0 + \left(\frac{\mu_s}{\mu_k} - 1.0\right)\mathrm{e}^{-\alpha|\dot{\delta}_1|}\right]\ \tanh(\sigma\dot{\delta}_1). \tag{6}$$

A value of 50 is chosen for the smoothening factor σ. Duan and Singh [1,2] have justified this choice by applying the same formulation and factor to a similar automotive drive train torsional system.

3. Pure slip transient response

Typical parameters for the reduced driveline system of Fig. 1(b) are: $I_1 = 0.2\ \mathrm{kg\,m^2}$, $I_2 = 0.02\ \mathrm{kg\,m^2}$, $C_{23} = 0.6\ \mathrm{Nm\,rad/s}$, $K_{23} = 3000\ \mathrm{Nm/rad}$, $A = 0.08\ \mathrm{m^2}$, $R = 0.1\ \mathrm{m}$, $\mu_s = 0.3$, $\mu_k =$

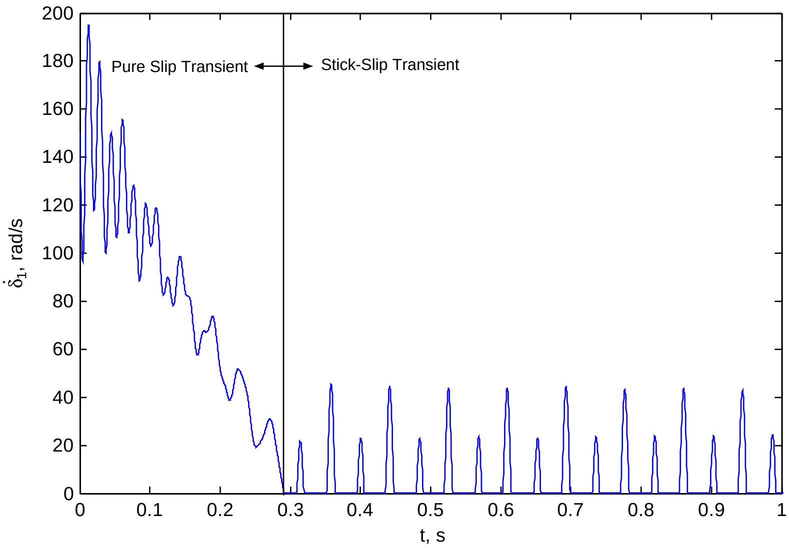

Fig. 2. Typical transient response for the 2-dof torsional system given $\omega = 150\cdot/\mathrm{s}$, $T_m = 300$; $T_p = 250$, $T_{sm} = 500$, $T_{sp} = 0.2T_{sm}$, $\omega_f = \omega$, $\psi = 0$, $\mu_k = 0.8\mu_k$ and $\Omega_e = 150\cdot/\mathrm{s}$.

$0.15 - 0.36$, $T_m = 300$ N m and $T_p = 250$ N m. First, observe a pure slip transient in Fig. 2 that results due to a speed difference between I_1 and I_2 during the initial engagement. Second, if we were to assume that only (pure) positive slip motions ($\dot{\delta}_1 > 0$) occur and that $\mu_k = \mu_s$ since the negative gradient dominates only when $\dot{\delta}_1$ approaches zero, Eqs. (2a,b) can be approximated as

$$I_1\ddot{\delta}_1 - \frac{I_1}{I_2}C_{23}\dot{\delta}_2 - \frac{I_1}{I_2}K_{23}\delta_2 + \left(1.0 + \frac{I_1}{I_2}\right)(T_{sm} + T_{sp}\ \sin(\omega_f t + \psi)) = T_m + T_p\ \sin(\omega t), \tag{7a}$$

$$I_2\ddot{\delta}_2 + C_{23}\dot{\delta}_2 + K_{23}\delta_2 = T_{sm} + T_{sp}\ \sin(\omega_f t + \psi). \tag{7b}$$

Assuming that I_1 rotates at the same speed as the engine and the rest of the driveline system stays still before any engagement process can take place, we obtain the following initial conditions:

$$\delta_1(0) = 0, \quad \dot{\delta}_1(0) = \Omega_e, \quad \delta_2(0) = 0, \quad \dot{\delta}_2(0) = 0. \tag{8a–d}$$

An analytical solution to Eq. (7b) is then given by a sum of complementary and particular solutions as

$$\delta_2(t) = \left\{\mathrm{e}^{-\varsigma\omega_n t}(a\ \cos(\omega_d t) + b\ \sin(\omega_d t))\right\} + \left\{\frac{T_{sm}}{K_{23}} + \frac{T_{sp}}{\sqrt{\Lambda}}\ \sin(\omega_f t + \psi + \phi)\right\}. \tag{9a}$$

$$\omega_n = \sqrt{K_{23}/I_2}, \quad \varsigma = C_{23}/\left(2\sqrt{K_{23}I_2}\right), \quad \omega_d = \omega_n\sqrt{1 - \varsigma^2}, \tag{9b–d}$$

$$\Lambda = (K_{23} - I_2\omega^2) + (C_{23}\omega)^2, \quad \phi = -\tan^{-1}(C_{23}\omega/(K_{23} - I_2\omega^2)). \tag{9e,f}$$

The constants a and b of Eq. (9a) are determined by applying the initial conditions (8c,d):

$$a = -\frac{T_{sm}}{K_{23}} - \frac{T_{sp}}{\sqrt{\Lambda}}\sin(\psi+\phi), \quad b = \frac{1}{\omega_d}\left\{a\varsigma\omega_n - \frac{T_{sp}}{\sqrt{\Lambda}}\omega_f\ \cos(\psi+\phi)\right\}. \tag{10a,b}$$

Substitute Eq. (10) into Eq. (7a) to yield the solutions for $\ddot{\delta}_1$ and $\dot{\delta}_1$, respectively, as

$$\begin{aligned}\ddot{\delta}_1(t) = {} & \frac{(T_m - T_{sm})}{I_1} + \frac{T_p}{I_1}\sin(\omega t) - \frac{T_{sp}}{I_1}\sin(\omega_f t + \psi) \\ & + \frac{T_{sp}}{\sqrt{\Lambda}}\omega_f^2 \sin(\omega_f t + \psi + \phi) \\ & + \mathrm{e}^{-\varsigma\omega_n t}\{(-a\omega_d^2 - 2\varsigma b\omega_n\omega_d + \varsigma^2\omega_n^2 a)\cos(\omega_d t) \\ & + (-b\omega_d^2 + 2\varsigma a\omega_n\omega_d + \varsigma^2\omega_n^2 b)\sin(\omega_d \tau)\},\end{aligned} \tag{11a}$$

$$\begin{aligned}\dot{\delta}_1(t) = {} & V_m + \frac{(T_m - T_{sm})}{I_1}t \\ & + \int\left\{\frac{T_p}{I_1}\sin(\omega t) - \frac{T_{sp}}{I_1}\sin(\omega_f t + \psi) + \frac{T_{sp}}{\sqrt{\Lambda}}\omega_f^2\ \sin(\omega_f t + \psi + \phi)\right\}\mathrm{d}t. \\ & + \int \mathrm{e}^{-\varsigma\omega_n t}\{(-a\omega_d^2 - 2\varsigma b\omega_n\omega_d + \varsigma^2\omega_n^2 a)\ \cos(\omega_d t) \\ & +(-b\omega_d^2 + 2\varsigma a\omega_n\omega_d + \varsigma^2\omega_n^2 b)\ \sin(\omega_d t)\}\ \mathrm{d}t.\end{aligned} \tag{11b}$$

The $\dot{\delta}_1(t)$ solution is further given in the following functional form, where the coefficients a_0, a_1, a_{21}, a_{22} and a_3 are defined by Eq. (11b):

$$\dot{\delta}_1(t) = a_0 + a_1 t + \{a_{21}\ \sin(\omega t + \varphi_{21}) + a_{22}\ \sin(\omega_f t + \varphi_{22})\} + a_3\mathrm{e}^{-\varsigma\omega_n t}\sin(\omega_d t + \varphi_3). \tag{12}$$

The above solutions lead to some interesting results. Under the situation when the amplitude of the oscillatory part is small and when the decaying component dies out quickly, the clutch engagement rate is controlled by a ramp of gradient $a_1 = (T_m - T_{sm})/I_1$. The time-varying friction torque T_{sp} contributes to the oscillatory motion during the ramp. Numerical results of Fig. 3(a) confirm the analytical functional forms of Eqs. (11b) and (12). As shown in Fig. 3(a), when T_m/T_{sm} is increased from 0.75 to 0.9, the ramp gradient decreases. Further, Fig. 3(b) shows the effects of I_1 from 0.2 to 0.4. Analytically, an increase in I_1 indicates more kinetic energy and thus the dissipation process should take more time. Conversely, when the oscillatory and decaying parts dominate the pure slip motion, it is difficult to determine the ramp gradient rate. Nonetheless, our analysis still gives a guideline regarding the value of $(T_m - T_{sm})$. As shown in Fig. 4, when T_m is higher than T_{sm}, no final engagement can be realized because the $a_1 t$ term in Eq. (12) would monotonically grow with time and ultimately it would dominate the response.

4. Stick-slip transient response (judder) and effect of harmonically varying dry friction

When $\dot{\theta}_2$ approaches $\dot{\theta}_1$ subsequent to the pure slip motion as discussed in the previous section, stick-slip transient motions would take place. In addition to introducing an objectionable noise problem, significant stick-slip torsional motions could be transferred by the differential to the

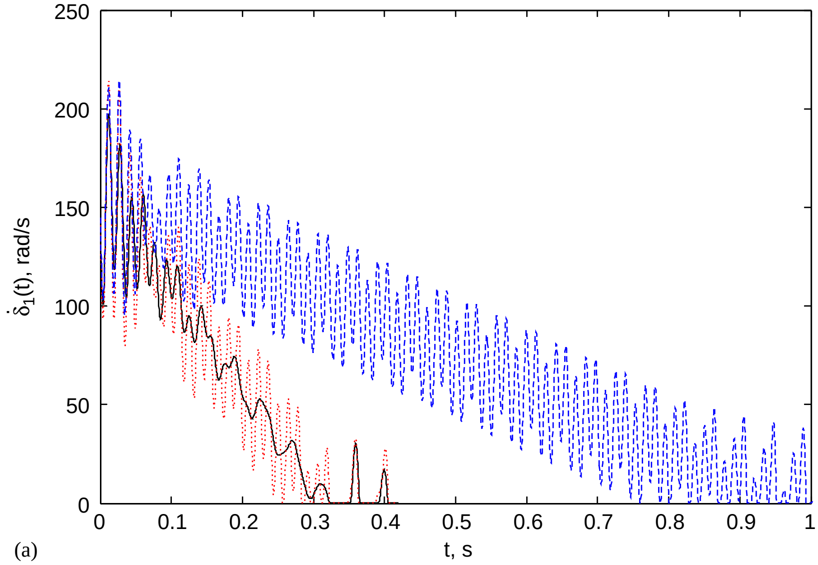

(a)

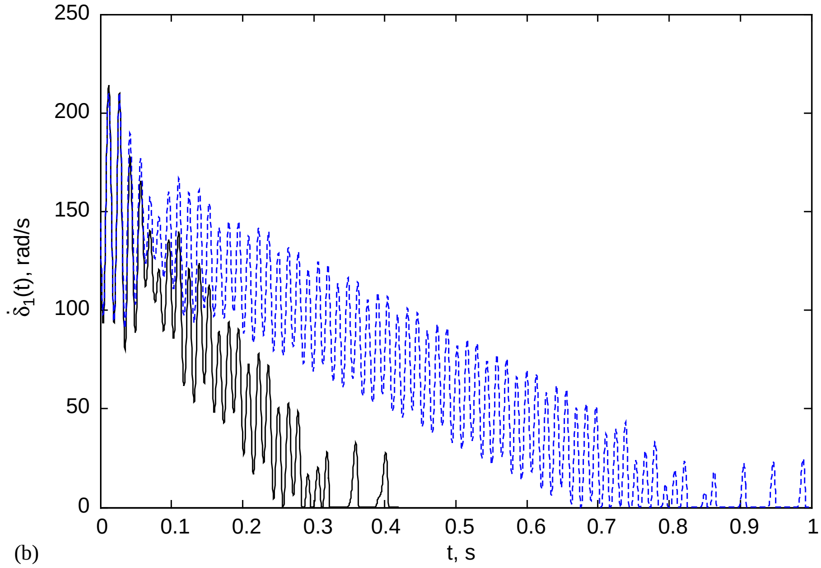

(b)

Fig. 3. Effect of the 2-dof system parameters on pure slip transients. (a) Effect of T_{sm}: —, $T_m/T_{sm} = 0.75$, $T_{sp} = 0$; · · ·, $T_m/T_{sm} = 0.75$, $T_{sp}/T_{sm} = 0.167$; – – –, $T_m/T_{sm} = 0.9$, $T_{sp}/T_{sm} = 0.167$. (b) Effect of I_1: —, $I_1 = 0.2$; – – –, $I_1 = 0.4$.

vehicle in the form of fore-after jerk. This phenomenon is usually referred to as the clutch judder problem that typically occurs at low frequencies [10]. Yamada and Ando [11] and Centea et al. [10] have called this the "negative damping" problem, introduced by the negative slope of $\mu_k(\dot{\delta}_1)$. Similar to their research, the negative slope of μ_k will be first investigated under a time-invariant friction torque T_{sm}. Then we will examine the effect of $T_s(t)$ under the $\mu_k = \mu_s$ assumption.

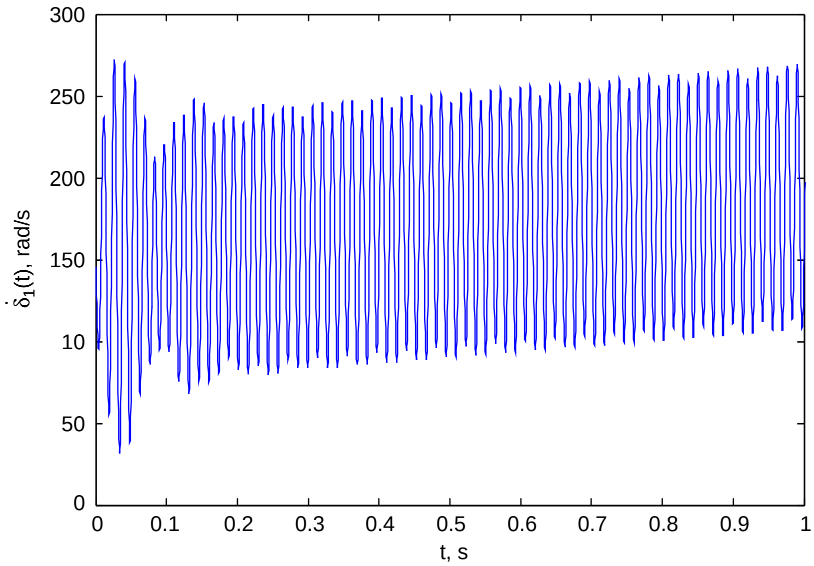

Fig. 4. Effect of T_{sm} on the clutch engagement in Fig. 2(b) given $T_m/T_{sm} = 1.05$ and $T_{sp}/T_{sm} = 0.5$.

From the friction formulation of Eq. (6), a decrease in μ_k with $\dot{\delta}_1$ affects the system in two ways. First, a negative slope regime is formed. Second, the saturation friction torque $T_{sm} = \mu_k$ ARP$_m$ is reduced and thus more slip motions are allowed. Fig. 5 shows results for three values of μ_k. As expected, the stick-slip motions become more pronounced when $\mu_k < \mu_s$, because the negative damping enhances the slip motions. Conversely, when $\mu_k > \mu_s$, the stick-slip motions are attenuated as a result of the positive damping as well as a higher value of T_{sm}, as seen in Fig. 5(a) and (b). To illustrate the effect of the negative slope more clearly, Fig. 6 compares the results for two cases of T_{sm} and μ_k. Note that although a reduction in T_{sm} would enhance the stick-slip motions, the negative slope characteristics ($\mu_k < \mu_s$) could further amplify them.

To examine the effect of harmonically varying friction torque on judder, first apply $T_s(t)$ at $\omega_f = \omega$, where ω is the frequency of engine torque $T_e(t)$, but with a phase lag of ψ. Results of Fig. 7(a) show that in-phase $T_s(t)$ tends to attenuate the stick-slip motions. A physical explanation can be found by analyzing the relationship between $T_e(t)$and $T_s(t)$ in a quasi-static manner as shown in Fig. 8(a). Note that only positive stick-slip motions ($\dot{\delta}_1 \geqslant 0$) are excited under a significantly high positive mean torque T_m. When the engine torque $T_e(t)$ is higher, say in the first half cycle ($\omega t \in [n2\pi\ n2\pi + \pi/2)$, $n =$ integer), the friction interface tends to initiate positive slipping motions. Quasi-statically, a higher value of T_s should suppress this tendency. But when there is a phase lag between T_s and T_e, such a suppression should be reduced. One could mathematically explain this by rewriting Eq. (7a) in the form

$$I_1\ddot{\delta}_1 - \frac{I_1}{I_2}C_{23}\dot{\delta}_2 - \frac{I_1}{I_2}K_{23}\delta_2 = \left[T_m - \left(1.0 + \frac{I_1}{I_2}\right)T_{sm}\right] + \left[T_p \sin(\omega t) - \left(1.0 + \frac{I_1}{I_2}\right)T_{sp} \sin(\omega t + \psi)\right]. \quad (13)$$

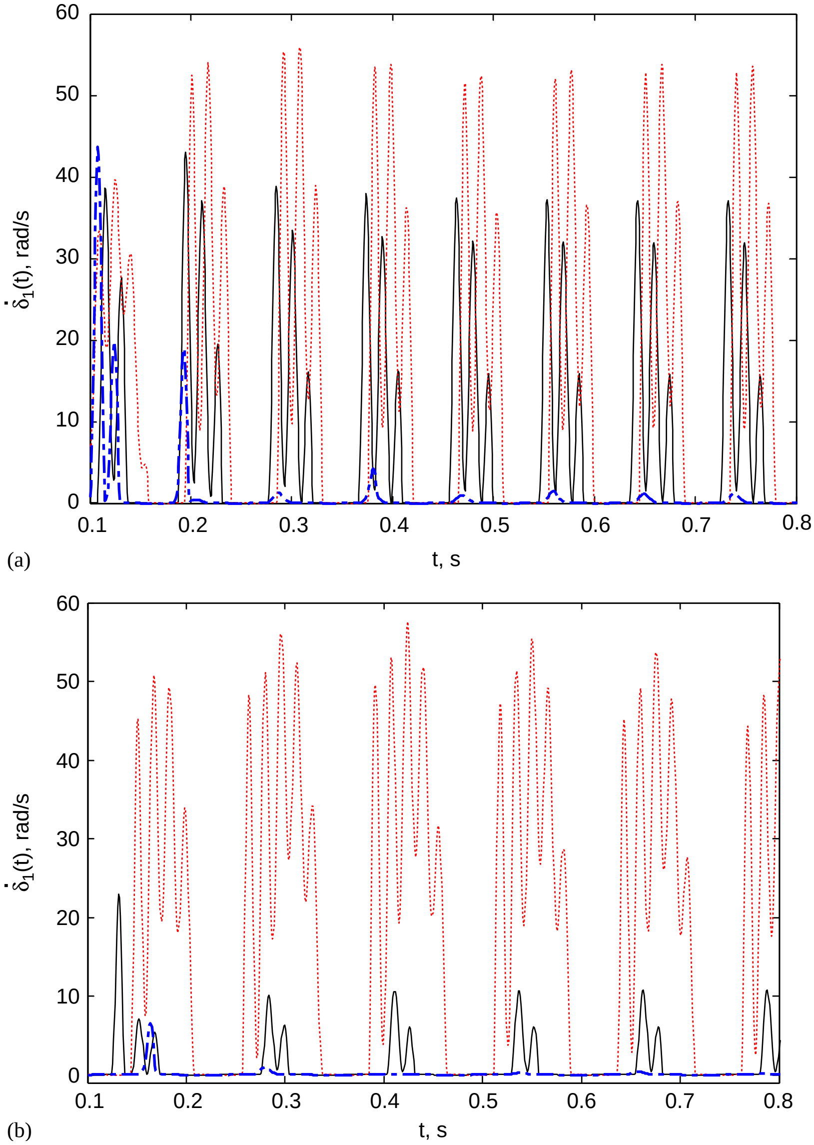

Fig. 5. Effect of μ_k on the transient stick-slip responses of a 2-dof system. (a) $\omega = 70\ \cdot/\mathrm{s}$ and $T_{sm} = 550\,\mathrm{N\,m}$; (b) $\omega = 50\ \cdot/\mathrm{s}$ and $T_{sm} = 550\,\mathrm{N\,m}$. Key: —, $\mu_k = \mu_s$; $\cdot\ \cdot\ \cdot$, $\mu_k = 0.75\ \mu_s$; $-\cdot-$, $\mu_k = 1.25\mu_s$.

As noted, when positive slipping tends to occur in the first half engine torque cycle, $\psi = 0$ provides the maximum decrease of the effective excitation as illustrated by the right-hand side of the above equation. This is consistent with the observation of Fig. 8(a).

Fig. 7(b) illustrates the case of mismatch between ω_f and ω. Observe that $T_s(t)$ with a mismatched frequency produces more slip motions. A similar physical explanation is presented in Fig. 8(b). Since $\omega_f \neq \omega$ and $\psi \neq 0$, some "leakage" as indicated by the shaded areas occurs and

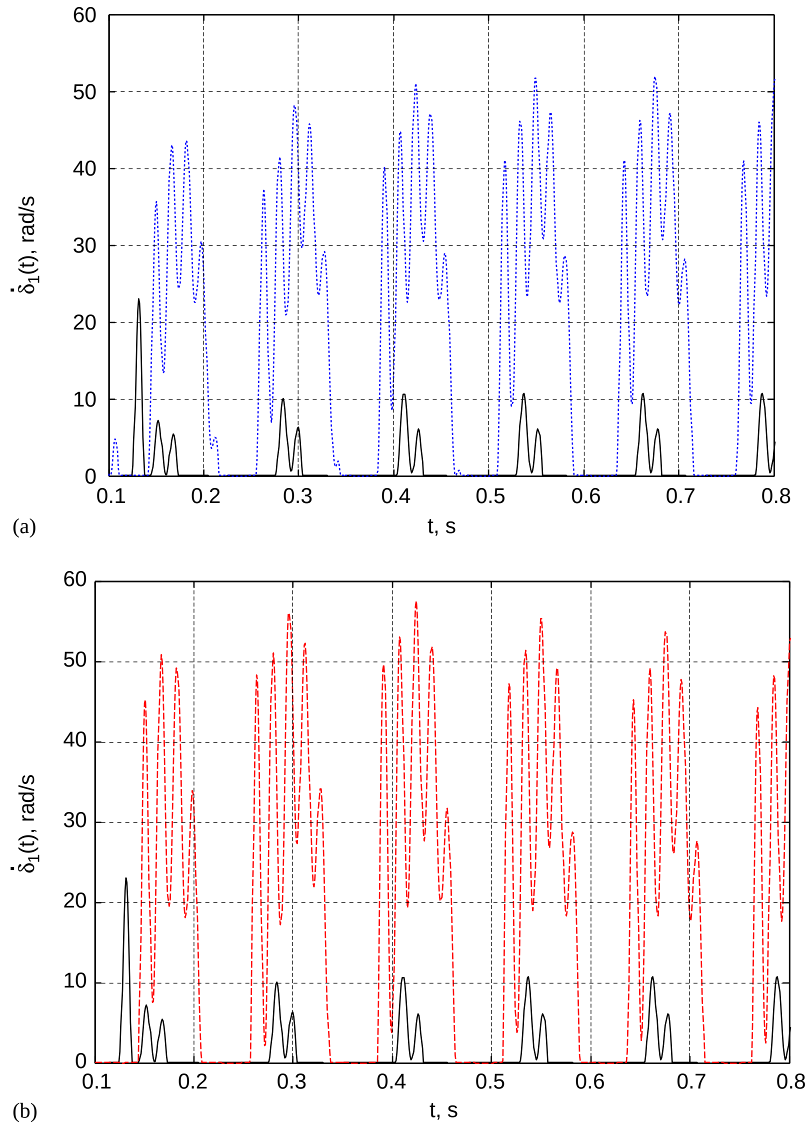

Fig. 6. Effect of reduced T_{sm} and negative slope in friction torque on the transient response of a 2-dof system when excited at $\omega = 50 \cdot /\mathrm{s}$. (a) —, $T_{sm} = 550\,\mathrm{N\,m}$, $\mu_k = \mu_s$; $\cdot\cdot\cdot$, $T_{sm} = 412.5$, $\mu_k = \mu_s$; (b) —, $T_{sm} = 550\,\mathrm{N\,m}$, $\mu_k = \mu_s$, – – –, $T_{sm} = 412.5\,\mathrm{N\,m}$, $\mu_k = 0.75\mu_s$.

consequently the slip motions are enhanced. Further, a time-varying $T_s(t)$ with $\omega_f = \omega$ and $\psi = 0$ is applied to a clutch with negative damping. Results of Fig. 9 show that $T_s(t)$ could efficiently reduce the judder problem in this case. Nonetheless, the explanation of Fig. 8 only applies at lower frequencies due to its quasi-static nature. As ω increases, phase delay between excitation and response may become important and the quasi-static explanation is no longer valid.

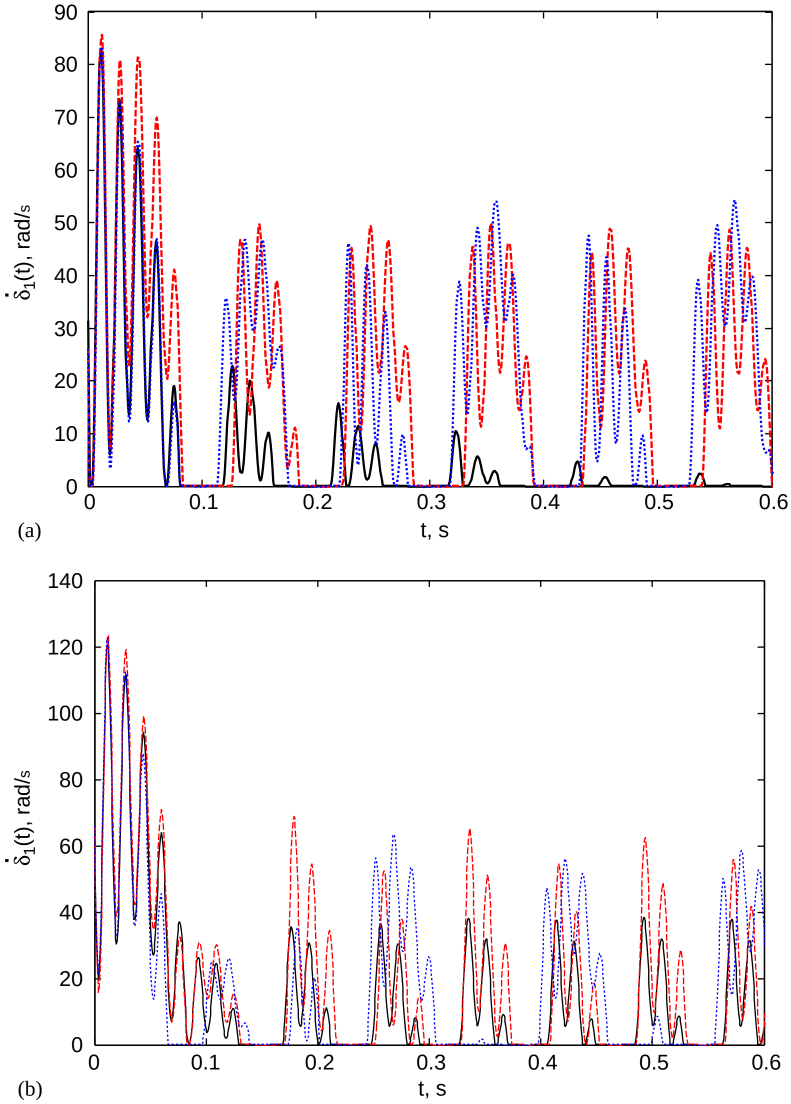

Fig. 7. Effect of harmonically varying friction on stick-slip transients of a 2-dof system. (a) Effect of phase lag ψ given $\omega = 60 \cdot /\mathrm{s}$ and $\omega_f = \omega$: —, $\psi = 0$, – – –, $\psi = \pi/2$, $\cdot\ \cdot\ \cdot$, $\psi = \pi$. (b) Effect of mismatched frequencies given $\omega = 80 \cdot /\mathrm{s}$ and $\psi = 0$: —, $\omega_f = \omega$; – – –, $\omega_f = 2\omega$; $\cdot\ \cdot\ \cdot$, $\omega_f = 0.5\omega$.

5. Conclusion

Specific effects of a significant dry friction path on the transient responses of a torsional system have been reported. An analytical solution for the pure slip motion is obtained based on a simplified linear system analysis. Our analyses show that three key parameters (T_m, T_{sm} and I_1) control the engagement rate within the friction interface. The $T_m \leqslant T_{sm}$ guideline has to be strictly followed to ensure the final engagement. The friction characteristics with a negative slope ($\mu_k < \mu_s$)

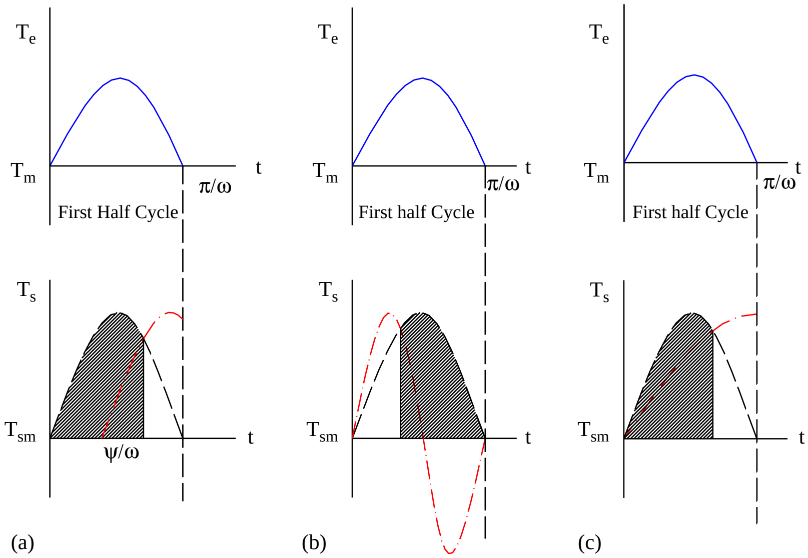

Fig. 8. Quasi-static explanation of the effect of harmonically varying friction torque on slip motions. All shaded areas represent the case for enhanced slip motions. (a) Effect of phase lag ($\omega_f = \omega$): —, $T_e(t)$; – – –, $T_s(t)$ in phase; – · –, $T_s(t)$ not in phase. (b) Effect of mismatched frequency ($\psi = 0$): —, $T_e(t)$; – – –, $\omega_f = \omega$; – – · – –, $\omega_f > \omega$. (c) Effect of mismatched frequency ($\psi = 0$): —, $T_e(t)$; – – –, $\omega_f = \omega$; – · –, $\omega_f < \omega$.

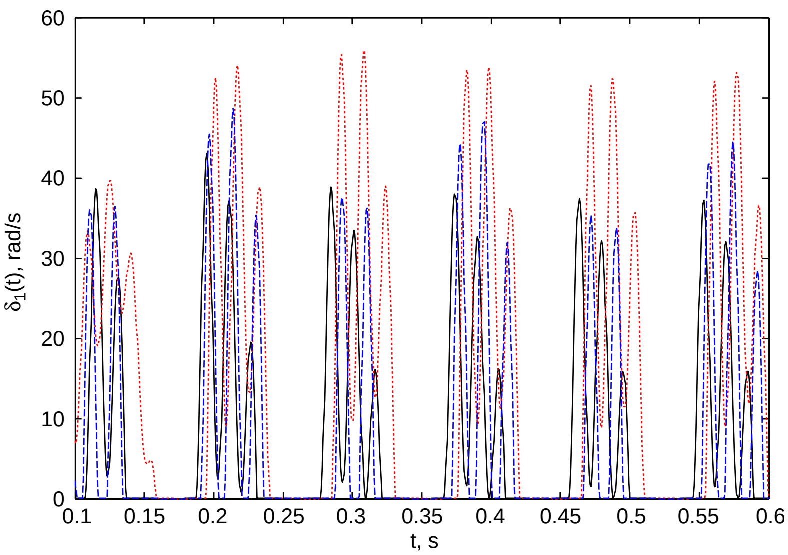

Fig. 9. Effect of harmonically varying friction $T_s(t)$ on clutch judder. Key: —, $\mu_k = \mu_s$ and $T_{sp} = 0$; · · ·, $\mu_k = 0.75\mu_s$ and $T_{sp} = 0$; – – –, $\mu_k = 0.75\mu_s$ and $T_{sp} = 1/3T_{sm}$.

are found to significantly affect the system dynamics in two ways: introduction of the "negative" damping effect and a reduction in the saturation friction torque. Although the negative damping may induce judder (substantial stick-slip motions), a well-tuned harmonically varying dry friction torque could possibly quench this behavior. Both physical and mathematical explanations have been proposed. Further studies will be reported in a subsequent article.

Acknowledgment

This research was supported by the DaimlerChrysler Challenge Fund.

References

[1] C. Duan, R. Singh, Super-harmonics in a torsional system with dry friction path subject to harmonic excitation under a mean torque, *Journal of Sound and Vibration* 285 (4+5) (2005) 803–834, this issue; doi:10.1016/j.jsv.2004.08.020.

[2] C. Duan, R. Singh, Stick-slip behavior in torque converter clutch, *SAE Noise and Vibration Conference*, Traverse City, MI, May 16–19, 2005, in review.

[3] J.P. Den Hortog, Forced vibrations with combined coulomb and viscous friction, *Transaction of the ASME*, APM-53-9, 1931, pp. 107–115.

[4] T.K. Pratt, R. Williams, Nonlinear analysis of stick/slip motion, *Journal of Sound and Vibration* 74 (4) (1981) 531–542.

[5] S.W. Shaw, On the dynamic response of a system with dry friction, *Journal of Sound and Vibration* 108 (2) (1986) 305–325.

[6] K. Kono, H. Itoh, S. Nakamura, K. Yoshizawa, Torque converter clutch slip control system, SAE Paper 950672, 1995.

[7] J. Hahn, K. Lee, Nonlinear robust control of torque converter clutch slip system for passenger vehicles using advanced torque estimation algorithms, *Vehicle System Dynamics* 37 (3) (2002) 175–192.

[8] E.J. Berger, Friction Modeling for dynamic system simulation, *Applied Mechanics Review* 55 (6) (2002) 535–577.

[9] J.R. Dormand, P.J. Prince, A family of embedded Runge–Kutta formulae, *Journal of Computational and Applied Mathematics* 6 (1) (1980) 19–26.

[10] D. Centea, H. Rahnejat, M.T. Menday, Non-linear multi-body dynamic analysis for the study of clutch torsional vibrations (Judder), *Applied Mathematical Modelling* 25 (2001) 177–192.

[11] N. Yamada, K. Ando, An analysis of clutch self-excited vibration in automotive drive line, SAE Paper 951319, 1995.